

Improvement of Wear and Corrosion Resistance of X46Cr13 Martensitic Stainless Steel by Cryogenic Treatment

I. Espinosa^{1,a*}, S. Menargues^{1,b}, D. Gutierrez^{1,c}, J.A. Picas^{1,d}, J. Navas^{2,e},
M.T. Baile^{1,f}

¹Department of Materials Science and Engineering, Universitat Politècnica de Catalunya (UPC), Spain

²Departament d'Enginyeria Gràfica i de Disseny (DEGD), Universitat Politècnica de Catalunya (UPC), Spain

^{a*}Isabel.Espinosa@upc.edu, ^bSergi.Menargues@upc.edu, ^cJoan.David.Gutierrez@upc.edu,
^dJosep.Picas@upc.edu, ^eJavier.Navas@upc.edu, ^fMaite.Baile@upc.edu

Keywords: cryogenic treatment, wear, AISI 420, martensitic stainless steel, electrochemical corrosion.

Abstract. This study investigates the effect of deep cryogenic treatment on the tribological and electrochemical performance of X46Cr13 martensitic stainless steel, with a particular emphasis on the synergistic interaction between wear and corrosion and its microstructural origins. The material was subjected to conventional quenching and tempering and compared with heat treatment routes incorporating cryogenic processing. Hardness measurements, wear tests, and electrochemical characterization by Tafel polarization were combined with quantitative microstructural analysis. Cryogenic treatment induces a pronounced microstructural refinement through the transformation of retained austenite into martensite and the enhanced precipitation of fine chromium-rich carbides, predominantly $M_{23}C_6$ and M_7C_3 . This process results in an increased carbide number density and a reduced average carbide area, leading to a more homogeneous carbide distribution within the martensitic matrix. The refined carbide population contributes to increased hardness and significantly improved wear resistance by effectively hindering plastic deformation and abrasive damage. Simultaneously, the stabilization of the martensitic matrix and the modified carbide–matrix interface promote the formation of a more uniform and stable passive film, improving corrosion resistance. The combined improvement in wear and corrosion behavior reduces the degradation rate under coupled mechanical and electrochemical loading, demonstrating a clear tribocorrosion synergy controlled by carbide characteristics. These findings highlight cryogenic treatment as an effective strategy for tailoring the microstructure of martensitic stainless steels to enhance their performance in aggressive and mechanically demanding environments.

1. Introduction

The aim of this study is to establish relations between microstructure, wear and corrosion resistance in a Martensitic Stainless-Steel heat treated in different methods.

There are applications for martensitic stainless steels in corrosion resistance, dental and surgical instruments, cutlery and the mining sector in wear -resistant parts due to the combination of corrosion, wear, and mechanical properties.

The uses of stainless-steel guarantee a remarkable corrosion resistance which derives from its content of chromium (>12 wt%) that forms a stable passivation layer of chromium oxide (Cr_2O_3) protecting the bulk against corrosion [1]

This study tries to clarify the differences in microstructural features and relations with wear and corrosion resistance, when a different heat treatment are applied in AISI 420. According to the literature the reasons for this are that the extent of microstructural changes may be different for each steel classes [2].

Key factors influencing the strength of martensitic stainless steel include the amount of dissolved carbon in the matrix, the size of martensite laths, the size and distribution of carbides, and dislocation density[3].

The effect of cryogenic treatment on the microstructure of steels has been extensively studied:

- Variations in the retained austenite amount and its other characteristics. The amount of austenite retained increases dramatically with increasing carbon content in room-temperature quenched carbon steel and its alloying elements dissolved.
- The refined martensitic sub-structure.
- Influence on the precipitation of nano-sized carbides during tempering.
- Additional small globular carbide (SGC) formation.

During the austenitization of martensitic stainless steels, the $(Cr,Fe)_{23}C_6$ carbides are dissolved, and the ferrite is transformed into austenite. The $(Cr,Fe)_{23}C_6$ carbides inhibit the grain growth of prior austenite grains [4].

As the tempering temperature increases, the dislocation density in the matrix decreases, and different carbides precipitate in the order of M_3C , M_7C_3 , and $M_{23}C_6$. [3]

Final microstructure will define tribological and electrochemical corrosion resistance.

2. Experimental

2.1. Materials and preparation

In this work the material studied was Martensitic stainless steel X46Cr13. The chemical composition is shown in Table 1.

Table 1. Chemical composition to X46Cr13 (wt%).

Element	Fe	C	Cr	Mn	Si	P	S
W%	85	0.44	13.7	0.86	0.29	0.029	0.005

X46Cr13 is an alloy composed of approximately 85–88% iron, 12–14% chromium, and 0.15–0.45% carbon. It offers high hardness and excellent wear resistance, making it suitable for cutting tools, medical instruments, industrial gears, and automotive components. This alloy includes variants such as 420J1 and 420J2.

Stainless steel X46Cr13 can be classified into several subgroups based on its carbon content and specific properties.

X46Cr13 stainless steel is used for cutlery, kitchen tools, and medical instruments due to its corrosion resistance. It is also used in industrial machinery and automotive parts, where durability and wear resistance are important.

2.2. Heat treatment

The heat treatment of X46Cr13 steel was defined according to industry practices outlined in ASM Handbook Vol. 4 – Heat Treating[5], as well as in technical guides from European manufacturers of martensitic stainless steels.

The cycle was adjusted to achieve a target hardness, prioritizing wear resistance. Corrosion behavior was evaluated in a Tafel test.

Several scientific articles have studied the effect of cryogenic treatment variables on the microstructure and improvement of mechanical properties, with deep cryogenic treatment being the best rated [6].

In accordance with the above, three different thermal cycles have been evaluated (Table 2).

Table 2. Applied heat treatment parameters.

Ref	Tempering Temp. [°C]	Cryogenization Tmep. / time [°C/ 4h]	1rst annealing Temp. [°C]	2on annealing Temp. [°C]
TR	1050	■	275	■
TRR	1050	■	275	275
TCR	1050	-196/4	275	■

Samples were named with the following acronyms, related to applied heat treatment: TR: Tempering and annealing; TRR: Tempering a doble annealing; TCR: Tempering + cryogenic treatment + annealing.

The studied material has been shaped by forging and provided by Matricir copany[7].

Heat treatments were performed using a Hobersal 12-PR/300 furnace for tempering and quenching. Tempering was carried out with oil, while cryogenic treatment consisted of immersion at $-196\text{ }^{\circ}\text{C}$ in liquid nitrogen.

3. Methods and Results

3.1. Microstructural features

Microstructural observations were conducted with a LEICA MEF 4M optical microscope and analyzed using NIS-Elements BR software. Furthermore, SEM analysis was performed to further characterize the microstructural features as shown in Figure1.

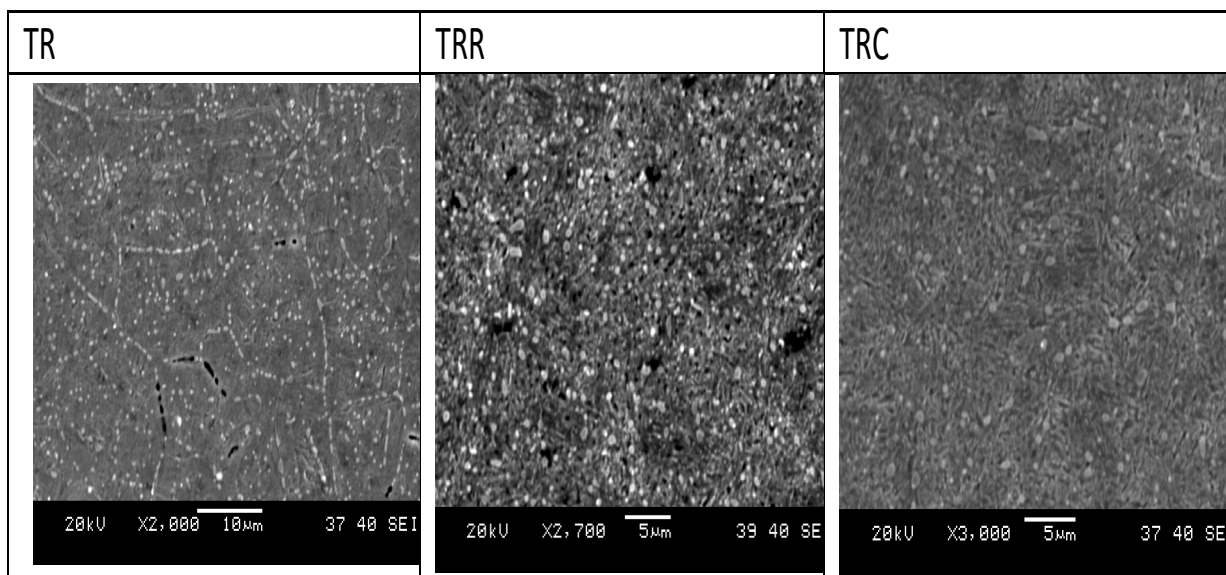


Fig. 1. X46Cr13. martensitic stainless steel. Microstructure of tempered martensite with intergranular and intragranular precipitates. Etched with Vilella. a) TR. b) TRR and c) TCR.

The SEM micrographs of the specimens after the heat treatments, Figure 1. showed the microstructure consisting of very fine lenticular martensitic matrix with globular carbides.

Several carbides may precipitate such as the M_2X , M_3C , M_7C_3 , $M_{23}C_6$, and MC types. It shows the refinement of carbide.

Plastic deformation during martensitic transformation at low temperatures is a key factor for the formation of carbon clusters that serve as nucleation sites for fine carbides. The martensitic transformation at low temperatures is accompanied by plastic deformation due to the volume effect of the martensitic transformation, which leads to the capture of immobile carbon atoms by gliding dislocations, generating carbon clusters. During tempering, these carbon clusters serve as nucleation sites for the precipitation of fine carbides.

In the following sequence of pictures, Figure 2 one can observe the difference in carbide density between TRR, TCR and TR heat treatments. Moreover, a reduction in particle size of carbides is also observed.

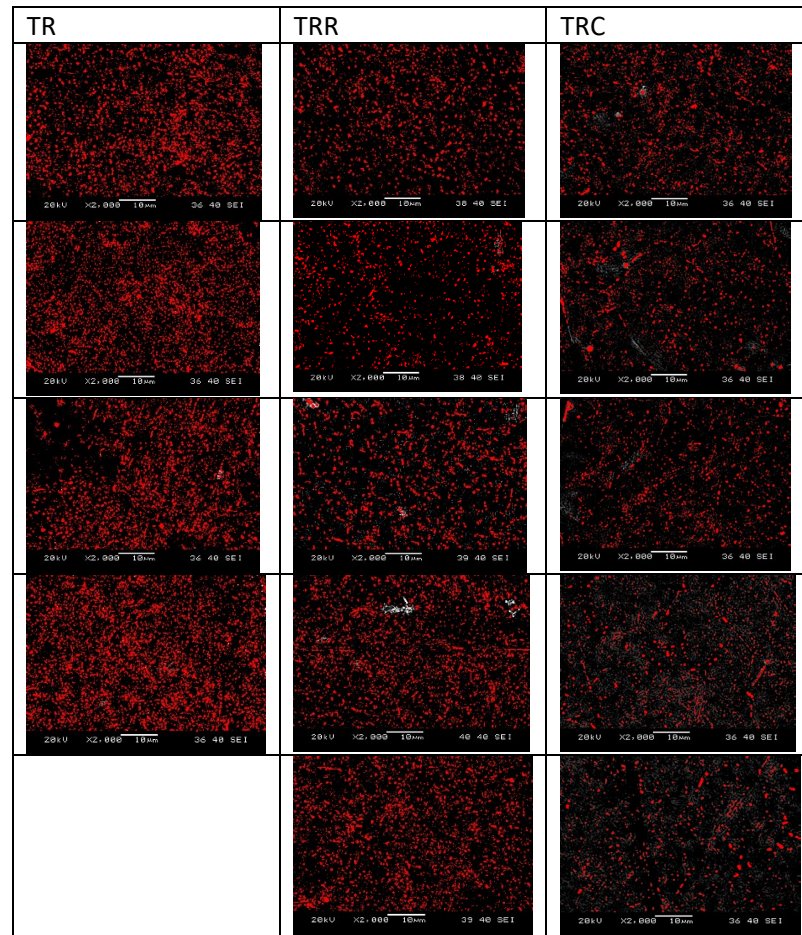


Fig. 2. Sequence of SEM micrographs for TR, TRR and TCR heat treated samples.

Figure 3 shows the evolution of the quantity and size of carbide precipitates for the different heat treatments carried out.

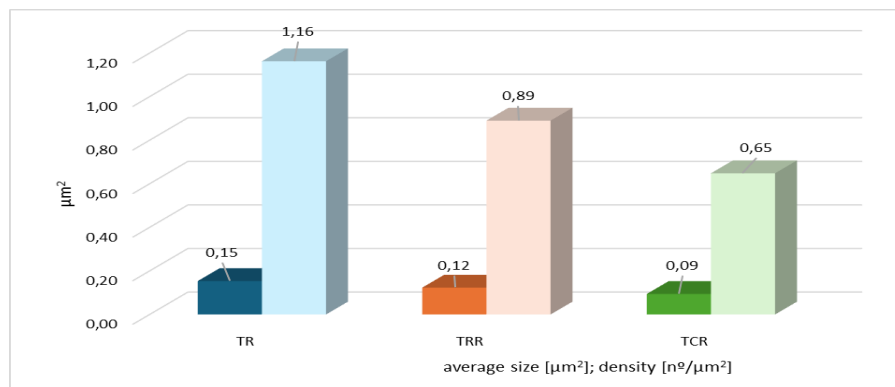


Fig. 3. Density and size of carbides are compared between of TR, TRR and TCR heat treatments.

Quantitative analysis of carbides revealed that the TCR treatment has the smallest average size (0.09 μm) and lower carbide density, which correlates with the lowest observed wear rate. In contrast, the TR treatment showed larger and denser carbides, associated with higher wear and poorer corrosion behavior.

In several studies an average carbide size reduction after the application of cryogenic treatments was reported [8]. In this work, the observed reduction was very relevant. TCR carbide average size decreases by 40% related to conventional treatment TR. In the case of TRR the decrease was 20%. TCR characteristic could be attributed to segregation of carbon atoms promoted by cryogenic treatment evolving to precipitation of carbides in subsequent tempering.[6]

Complementary data obtained by X-ray diffraction (XRD), a presence of 8% retained austenite in the TR specimen.

3.2. Hardness

The hardness was measured on a polished mirror surface of the material by using a Duramin5 microhardness tester (Struers) with a Vickers diamond indenter under an applied load of 300gf, according to ASTM E384 standard (HV0.3). Thirty data points were collected and averaged for each hard result.

Table 3. Average HV0.3 values for TR, TCR and TRR samples.

	HV0.3	Hardness variation
TR	605	
TCR	617	+ 2%
TRR	515	-15%

As shown in Table 3, the hardening response of AISI 420 is not significantly influenced by the cryogenic treatment. In contrast, the reduction in hardness observed after applying double tempering is significant.

It has been widely reported that cryogenic treatment can promote the transformation of retained austenite into martensite in steels, whereas precipitation of carbides may have little contribution to improved hardness [6].

Tempering is widely used to relax the martensitic microstructure, promoting carbon diffusion and carbide nucleation; therefore, the resulting hardness reduction is very common.

3.3. Tribological properties

Tribological performance under dry sliding conditions was evaluated using a Pin-on-disc tribometer (CSM Instruments), following ASTM G99-23 wear testing standards. Samples were ground and polished to a 1 μm diamond finish. Tests were performed with a 6 mm alumina pin sliding against the polished specimens at 0.10 $\text{m}\cdot\text{s}^{-1}$ under an applied load of 10 N applied load. Experiments were conducted at 25 $^{\circ}\text{C}$ and $\sim 50\%$ relative humidity. After a sliding distance of 0.8 km, material loss was determined by measuring the cross-sectional area of wear tracks with a profilometer (Taylor–Hobson Form Talysurf Plus roughness tester).

In Figure 4 a schematic Pin- On – Disc is shown.

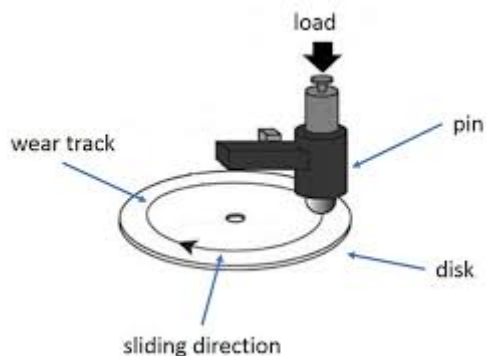


Fig. 4. Schematic drawing of the Pin-on-disc; Image from Pin- On- Disc used in the trials.

In Figure 5.- can be seen no statistically significant differences were observed in the friction coefficient between treatments, suggesting that wear resistance is predominantly influenced by microstructural modifications rather than changes in surface friction.

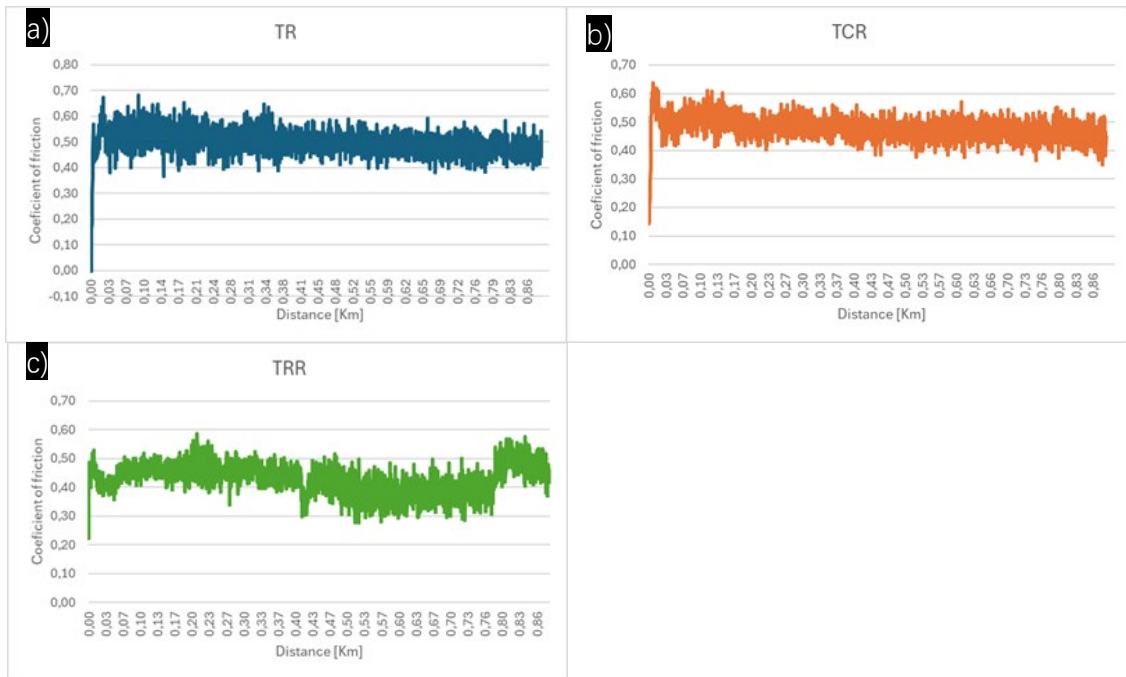


Fig. 5. Coefficient of friction for different Heat Treatment a) TR, b) TRC and c) TRR.

In terms of Specific Wear Rate [$\text{m}^3 \cdot (\text{N} \cdot \text{m})^{-1}$], Fig 6 shown dry pin-on-disc tests showed that the TCR treatment had the lowest specific wear rate (65% lower respect TR), followed by TRR (34.4 % lower respect TR) and TR.

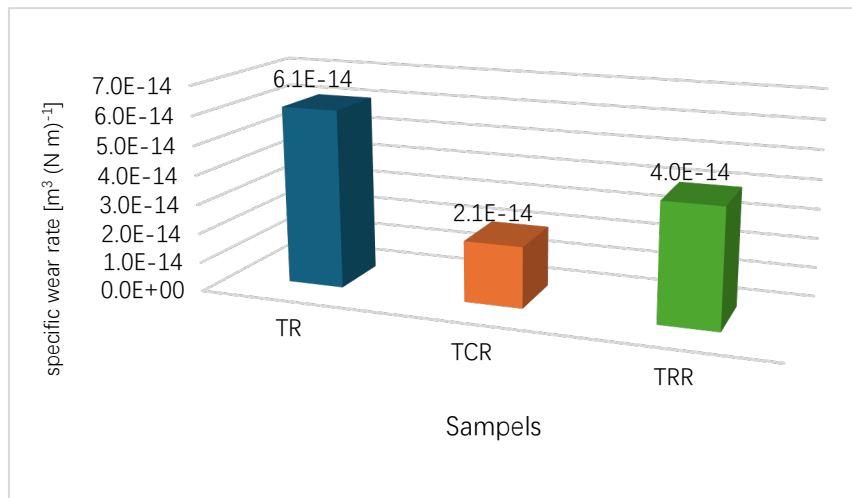


Fig. 6. Values for specific wear rate [$\text{m}^3 (\text{N} \cdot \text{m})^{-1}$] obtained in pin-on-disc test.

In Figure 7 wear track of TR (a, b) and TCR (c, d) sample after the wear test is shown. It is observed difference in wear mechanism for different heat treatment. As could be seen, sever adhesion took place during sliding, with a high amount of plastic deformation of the surface and plate-like debris in the surrounding of the wear track. The worn surface appears to be metallic, without signs of oxidation.

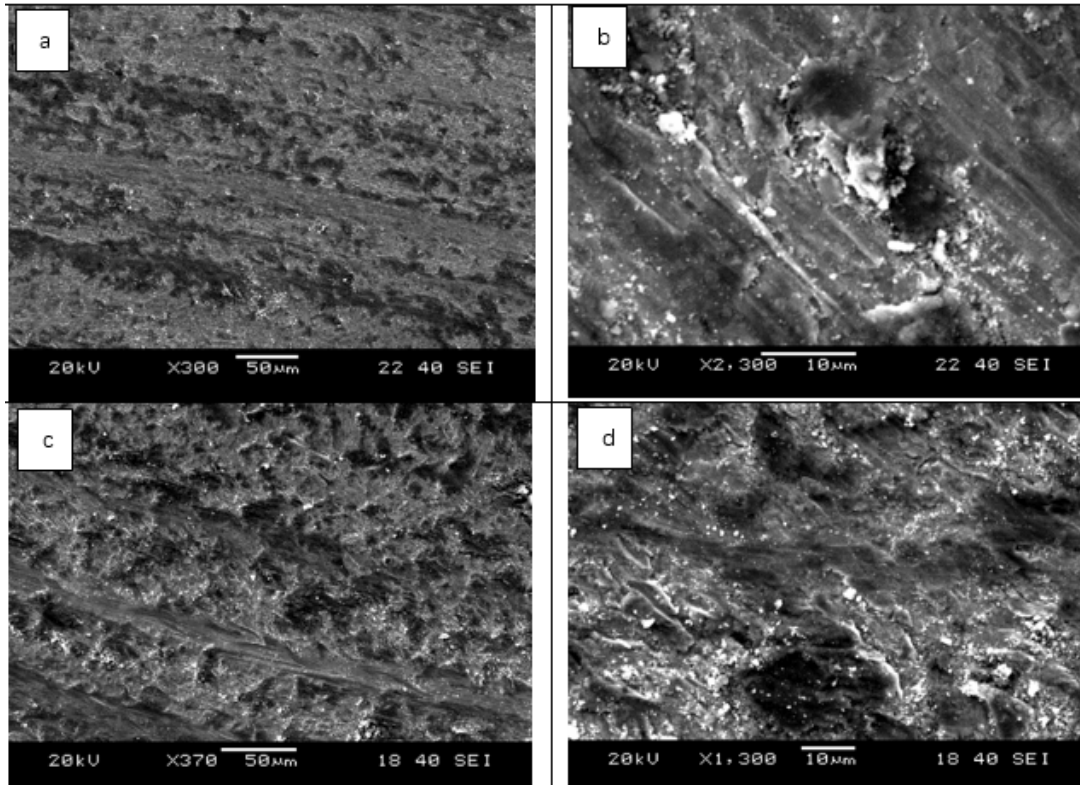


Fig. 7. Micrographics SEM, appearance of the wear channel. A and B for TR and Cand D for TCR.

Although all samples exhibited comparable coefficients of friction, significant differences were observed in their wear responses as a function of the heat treatment. The quenched and tempered condition showed a predominantly severe abrasive wear mechanism, evidenced by deep and continuous grooves aligned with the sliding direction, together with localized adhesive damage and material removal. In contrast, the cryogenically treated and tempered samples presented a noticeably milder wear regime, characterized by shallower grooves and a more uniform worn surface, indicating a transition from micro-cutting to micro-ploughing. The reduced occurrence of adhesive features and surface delamination suggests improved microstructural stability during sliding. This enhanced wear resistance is attributed to the reduction of retained austenite and the increased stability of the martensitic matrix promoted by the cryogenic treatment, which effectively limits plastic deformation and material loss.[9]

While adhesive wear resistance mainly requires higher hardness, abrasive wear also requires primary carbides[10].

3.4. Corrosion resistance

Electrochemical tests were carried out using a Bio-Logic VMP3 potentiostat with EC-Lab V9.52 software, employing a three-electrode cell in a 3.5% NaCl electrolyte.

Thermodynamic parameters were determinate: corrosion potential E_{corr} and Corrosion current I_{corr} , Tafel constants β_a (anodic coefficient) and β_b (cathodic coefficient), the corrosion rate.

Corrosion rate has been determinate using the following equation:

$$V_{\text{corr}} = \frac{K i_{\text{corr}} EW}{\rho} \quad (1)$$

Where: V_{corr} : corrosion rate ($\text{mm} \cdot \text{year}^{-1}$); I_{corr} : corrosion current density ($\mu\text{A} \cdot \text{cm}^{-2}$); EW: equivalent weight of the metal; ρ : metal density; K: constant $0.00327 \text{ mm} \cdot \text{year}^{-1}$

In Table 4 It can be the obtained values.

Table 4. Obtained values for electrochemical test using Eq.1.

Sample	E _{corr} [mV]	I _{corr} [μ A/cm ²]	B _c	B _a	Chi ²	equivalent weight [g/eq]	density [g/cm ³]	surface area [cm ²]	corrosion rate [mm/year]
TCR 0	-337,06	1,03	199,39	146,37	224,55	27,6	7,7	0,78	0,0155
TCR 1	-308,84	0,36	122,44	158,80	306,10	27,6	7,7	0,78	0,0054
TCR 2	-310,80	0,90	140,53	166,83	612,24	27,6	7,7	0,78	0,0136
TR 0	-476,34	2,41	238,01	95,57	32,33	27,6	7,7	0,78	0,0362
TR 1	-368,59	3,67	216,69	71,11	221,31	27,6	7,7	0,78	0,0551
TR 2	-445,11	2,58	249,52	101,49	91.155,70	27,6	7,7	0,78	0,0388
TRR 0	-302,44	0,55	150,16	84,81	52.044,00	27,6	7,7	0,78	0,0083
TRR 1	-297,30	0,45	1.119,92	114,24	3.558,01	27,6	7,7	0,78	0,0068
TRR 2	-370,68	1,39	178,00	90,80	6.803,53	27,6	7,7	0,78	0,0209

To evaluate the comparative *corrosion rate* a simple representation is done in figure 8.

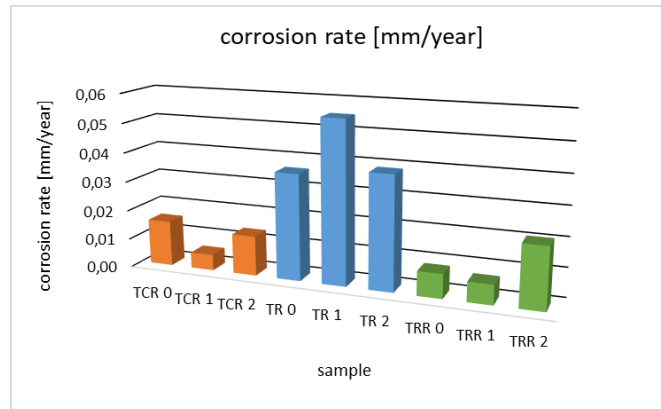


Fig. 8. Comparative values representation for corrosion rate according to different applied heat treatment.

The double tempering treatment (TRR) showed the lowest corrosion rates, mainly due to reduced residual stresses and a more uniform chromium distribution in the matrix, thereby enhancing the formation of a more stable passive film. The TCR treatment showed intermediate behavior, while the TR treatment showed higher corrosion rates, associated with a less stable microstructure and greater chemical heterogeneity.

The potentiodynamic polarization curves represented in Figure 9, show that the TRR treatment shifts the corrosion potential towards more noble values and reduces the corrosion current density compared to TR and TCR. This behavior is associated with a more stable microstructure, with a lower defect density and a more homogeneous distribution of chromium in the matrix favoring the formation of a more protective passive film. These results are according to the literature.[11]

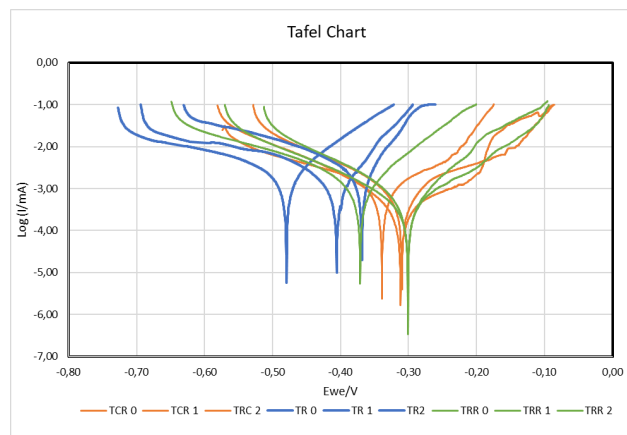


Fig. 9. Polarization curves for different applied heat treatments.

Fig 10 shows the corrosion surfaces corresponding to the three heat treatments after being exposed to an electrochemical corrosion test. In all cases, the predominant corrosion mechanism is pitting

corrosion, which initiates in chromium-depleted zones around chromium carbides. These areas act as weak points in the passive layer, leading to a reduction in the pitting potential.

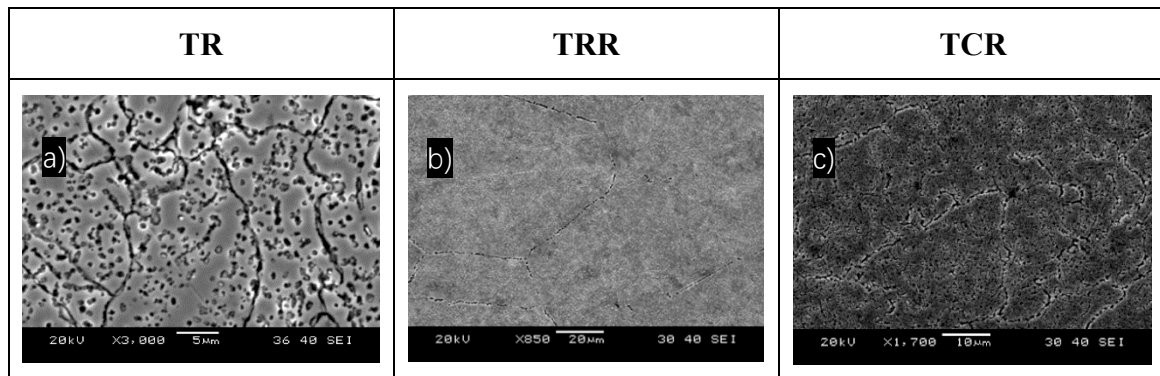


Fig. 10. SEM micrographs of the specimens after the corrosion tests. a) TR, b) TRR and c) TCR.

4. Conclusion

- Cryogenic treatment has no significant influence on hardness, probably because the little fraction of retained austenite, also happens in term of friction coefficient. The significantly improvement in wear resistance of the steel could be attributed to segregation of carbon atoms promoted by cryogenic treatment evolving to precipitation of carbides. This characteristic is well founded in microstructural results.
- The TRR heat treatment provides the best corrosion resistance in AISI 420, followed by TCR, while the TR treatment shows the least favorable behavior.
- The refinement in carbide size and homogeneous distribution generated in cryogenic and double tempering was sufficiently notable to improve wear resistance of a low-carbon AISI 420 stainless steel.
- Because the retained austenite in AISI 420 TR has been so low, the improvements in wear have been attributed to refinement and homogeneous distribution for carbides.
- Could be assume the chromium depletion zone size thicken with the bigger are the carbides, so the corrosion potential and the corrosion rate increase.
- Less density of carbides helps less spots for the passive layer, and could be indicated the matrix has a higher percentage of dissolved Cr. Following this argument, TRR and TCR heat treatments are more corrosion resistance than TR.
- A positive correlation was observed between the average carbide size and the specific wear rate, indicating that larger carbides favor micro-tearing and delamination mechanisms.
- The TRR treatment represents an intermediate condition, offering a compromise between wear resistance and corrosion resistance.

The greater hardness and lower specific wear rate observed in the TCR samples are associated with a more refined microstructure, characterized by smaller carbides and a lower fraction coefficient of retained austenite. In contrast, the TRR treatment, despite exhibiting the lowest hardness, showed the best corrosion resistance, highlighting the trade-off between wear resistance and corrosion resistance in X46Cr13 steel.

The average carbide size primarily governs wear resistance, while carbide density more directly influences corrosion behaviour, demonstrating that different microstructural parameters control different degradation mechanisms in X46Cr13 martensitic stainless steel.

Future work will focus on establishing quantitative correlations between grain size, carbide morphology, and passive film stability to provide deeper insight into the microstructural control of corrosion and tribocorrosion resistance.

References

- [1] M. Maher, I. Iraola-Arregui, H. Ben Youcef, B. Rhouta, and V. Trabadelo, “The synergistic effect of wear-corrosion in stainless steels: A review,” in *Materials Today: Proceedings*, Elsevier Ltd, 2021, pp. 1975–1990. doi: 10.1016/j.matpr.2021.05.010.
- [2] P. Jurči and I. Dlouhý, “Cryogenic Treatment of Martensitic Steels: Microstructural Fundamentals and Implications for Mechanical Properties and Wear and Corrosion Performance,” Feb. 01, 2024, *Multidisciplinary Digital Publishing Institute (MDPI)*. doi: 10.3390/ma17030548.
- [3] H. J. Chen *et al.*, “Effects of heat treatment on microstructure, mechanical properties and corrosion resistance 13Cr-2Ni-2Mo martensitic stainless steel,” *Mater. Charact.*, vol. 223, May 2025, doi: 10.1016/j.matchar.2025.114909.
- [4] A. N. de Moura *et al.*, “Effect of austenitization temperature on microstructure, crystallographic aspects, and mechanical properties of AISI 420 martensitic stainless steel,” *Materials Science and Engineering: A*, vol. 909, Sep. 2024, doi: 10.1016/j.msea.2024.146835.
- [5] K H PRABHUDEV, *Handbook of Heat Treatment of Steels*. 1992.
- [6] R. F. Barron, “Cryogenic treatment of metals to improve wear resistance,” *Cryogenics (Guildf)*., vol. 22, no. 8, pp. 409–413, Aug. 1982, doi: 10.1016/0011-2275(82)90085-6.
- [7] Disponible a: <https://matricir.com/>, “Matricir | Fabricación de matrices y rodillos a medida.”
- [8] J. Anna Sajan, R. Reji, and A. Mohamed Rafi, “A Review on the Cryogenic Treatment of Stainless Steels, Tool Steels and Carburized Steels,” Jun. 2020. [Online]. Available: www.ijisrt.com.
- [9] A. Dalmau, C. Richard, and A. Igual – Muñoz, “Degradation mechanisms in martensitic stainless steels: Wear, corrosion and tribocorrosion appraisal,” *Tribol. Int.*, vol. 121, pp. 167–179, May 2018, doi: 10.1016/j.triboint.2018.01.036.
- [10] Ph. D. F. George E. Totten, “Steel Heat Treatment - Metallurgy And Technologies,” no. Metallurgy and technologies, 2006.
- [11] S. Van Der Meer, “Rijksuniversiteit Groningen Effect of Heat Treatment and Composition on Electrochemical Behaviour of AISI 420 Martensitic Stainless Steels,” 2016.